

**Original Research**

## Synovial and pulmonary dysfunctions are induced by crosstalk of Smad and Erk pathways in an arthritis model

Wan Lei<sup>1</sup>, Liu Jian<sup>1\*</sup>, Huang Chuanbing<sup>1</sup>, Chen Xi<sup>1</sup>, Liu Lei<sup>1</sup>, Liu Tianyang<sup>1</sup>, Ge Yao<sup>1</sup>, Fan Haixia<sup>1</sup>, Zhao Lei<sup>2</sup>, Li Zhnege<sup>3</sup><sup>1</sup> The First Affiliated Hospital of Anhui University of Chinese Medicine, Hefei 340031, China<sup>2</sup> Anhui University of Chinese Medicine, Hefei 340031, China<sup>3</sup> Department of Cancer Biology, City of Hope National Medical Center and Beckman Research Institute, California 91010, USA\*Correspondence to: [liujianahzy@126.com](mailto:liujianahzy@126.com)

Received November 12, 2019; Accepted April 18, 2020; Published May 15, 2020

Doi: <http://dx.doi.org/10.14715/cmb/2020.66.2.2>

Copyright: © 2020 by the C.M.B. Association. All rights reserved.

**Abstract:** In the current experiment, the effects of transforming growth factor (TGF)- $\beta$ 1/Smad and ERK pathway crosstalk on synovial and pulmonary systems during rheumatoid arthritis have been investigated. For this purpose, rats were divided into normal control (NC) and model control (MC) groups. In the MC group, 0.1 ml Freund's complete adjuvant was injected intradermally into the right hind paw, and the resulting inflammation represented a rheumatoid arthritis model. Joint swelling and changes in lung functions were observed in arthritic rats. Synovial and lung were observed by light and electron microscopies. Enzyme-linked immunosorbent assays were used to detect TGF- $\beta$ 1, interleukin (IL)-1 $\beta$ , IL-4, IL-10, interferon- $\gamma$  (IFN- $\gamma$ ), connective tissue growth factor (CTGF), and fibroblast growth factor (FGF). PCR, immunohistochemistry, and immunoblotting were used to detect changes in Smad and ERK pathways of synovial and lung tissues. Compared with the NC group, toe swelling was elevated in the MC group. Pulmonary functions FEV1, FEF50, FEF75, MMF, and PEF were decreased ( $P < 0.01$ ). Serum cytokines IL-1 $\beta$ , IL-4, TGF- $\beta$ 1, and CTGF were increased, while IFN- $\gamma$ , IL-10, Th1/Th2 cell ratio, and FGF were decreased ( $P < 0.01$  or  $P < 0.05$ ). Expression of *TGF- $\beta$ 1* and *Smad2/3/4 mRNAs* and TGF- $\beta$ 1, T $\beta$ RI, T $\beta$ RII, Smad2/3, p-Smad2/3, and Smad4 proteins in the synovial membrane and lung tissue were increased, and expression of *Smad7 mRNA* and protein was decreased ( $P < 0.01$  or  $P < 0.05$ ). Expression of *ERK2 mRNA* and p-ERK1/2 protein was increased in the synovial membrane and lung tissue, and expression of *ERK1/2 mRNAs* and ERK1/2 and p-ERK1/2 proteins was increased in lung tissue ( $P < 0.01$  or  $P < 0.05$ ). Correlation analysis showed that FEV1 was negatively correlated with TGF- $\beta$ 1 mRNA and protein in arthritic rats, FEF25 was negatively correlated with Smad4 protein, and FEF50 was negatively correlated with the T $\beta$ RII protein, and FEF75, *TGF- $\beta$ 1* and *Smad3 mRNAs*. There was a negative correlation between Smad2/3 protein and a negative correlation between PEF and TGF- $\beta$ 1 protein ( $P < 0.05$ ). FEF50 and MMF were positively correlated with *Smad7 mRNA* ( $P < 0.05$ ). FEV1 was negatively correlated with *ERK2 mRNA*, and FEF25 was negatively correlated with p-ERK1/2 protein. FEF75 and MMF were negatively correlated with ERK1/2 and p-ERK1/2, respectively ( $P < 0.05$ ). *ERK1 mRNA* was positively correlated with *Smad3 mRNA* and T $\beta$ RII protein, *ERK2 mRNA* was positively correlated with p-Smad2/3, and ERK1/2 protein was positively correlated with *Smad2 mRNA*, Smad4 protein, p-ERK1/2 protein, *Smad4 mRNA*, and p-Smad2/3 protein ( $P < 0.05$ ). p-ERK1/2 protein was negatively correlated with Smad7 protein ( $P < 0.05$ ). It is concluded that arthritic rats have synovial and systemic pulmonary damage. Smad and ERK pathway crosstalk leads to systemic lesions. Smad and ERK pathways are gradually activated by phosphorylation under the induction of the TGF- $\beta$ 1 promoter, and then participate in transcriptional activities, leading to the increase in synovial inflammation of arthritis, pulmonary lesions, and decreases in lung functions.

**Key words:** Rheumatoid arthritis; Arthritis; Lung function; TGF- $\beta$ 1/Smad pathway; ERK1/2 pathway.

### Introduction

Rheumatoid arthritis (RA) can cause damage to articular cartilage and bone. The basic pathological manifestations of RA are synovitis and vasculitis. RA lesions occur in joints as well as other tissues and organs. Because lungs are rich in connective tissue and blood vessels, lung tissue is more likely to be affected and secondary to lung lesions. RA lung lesions include pulmonary interstitial fibrosis, pleurisy, pulmonary vasculitis, and pulmonary hypertension (1-5). Studies have found that the incidence of lung involvement in RA patients with disease duration of more than 8 years is as high as 50% (6-9). About 70.5% of patients with RA lung lesions have pulmonary interstitial lesions, causing pulmonary interstitial fibrosis (10-11). RA pulmonary interstitial fibrotic lesions are characterized by a sudden onset,

rapid progression, and high mortality, which seriously affect the quality of life of RA patients. The early stage of RA pulmonary interstitial fibrosis changes to alveolitis that can progress to interstitial fibroblast proliferation, massive extracellular matrix deposition, coughing, wheezing, shortness of breath, chest tightness, and other difficulties in breathing. However, the early clinical manifestations of RA lung lesions are mild or atypical, and imaging indicators such as X-ray and CT often show no significant changes. Pulmonary function changes are advanced in the clinical manifestations of the respiratory system and chest imaging abnormalities (12-13). Therefore, because of the early or no atypical symptoms of RA lung disease, diagnosis is easily missed. Thus, it is necessary to systematically and deeply study the detrimental changes in lung functions of RA. A previous study has found that pulmonary function parameters FVC,

FEV1, MVV, FEF25, FEF50, FEF75, VC and PEF are significantly low in active RA patients (14). Therefore, it is of great importance to study RA lung lesions by observing changes in lung functions of patients.

## Materials and Methods

### Animals

Specific pathogen-free male Wistar rats were obtained from the Experimental Animal Center of Anhui Province (license number: SYXK (wan) 2005-02). Standard clean animal house. Freund's complete adjuvant (FCA) was prepared from Sigma (United States). Interleukin (IL)-1 $\beta$ , IFN- $\gamma$ , IL-4, IL-10, and TGF- $\beta$ 1 ELISA Kits were purchased from R&D (United States). A Trizol kit was purchased from Invitrogen (United States). Rabbit anti-TGF- $\beta$ 1, -Smad, and -ERK antibodies were purchased from Bioworld Biotechnology (United States).

### Model establishment

Rats were divided into normal control (NC) and model control (MC) groups MC group rats were injected with 0.1 ml FFA into the right hind paw to cause inflammation and establish the RA model.

### Observation of main indicators

#### Pulmonary function test

Pulmonary function parameters included forced vital capacity (FVC), first-second forced expiratory volume (FEV1), the maximum expiratory flow of 25% of vital capacity (FEF25), the maximum expiratory flow of 50% of vital capacity (FEF50), 75% of vital capacity, the maximum expiratory flow (FEF75), the maximum expiratory mid-flow (MMF), and the maximum expiratory flow (PEF). A software analysis system was used for data acquisition, real-time analysis and control, curve dynamic display, trend graphing, lung function parameter data conversion, and storage.

#### Detection of serum IL-1 $\beta$ and other cytokines by ELISAs

Serum IL-1 $\beta$ , IFN- $\gamma$ , IL-4, IL-10, TGF- $\beta$ 1, CTGF, and FGF were determined by ELISAs, according to the ELISA Kit protocols. The ratio of IFN- $\gamma$  to IL-4 indicated that of Th1 to Th2 cells (15-20).

#### Detection of TGF- $\beta$ /Smad and ERK mRNAs in synovial and lung tissues by RT-PCR

According to the gene sequences in GenBank, TGF- $\beta$ 1 (NM-021578), Smad2 (NM-019191), Smad3 (NM-013095), Smad4 (NM-019275), Smad7 (NM-030858), ERK1 (M61177), ERK2 (M64300), and internal reference GAPDH (NM 017008) primers were designed using Primer Premier 5.0 software. Primers were as following: TGF- $\beta$ 1 F primer 5'-CTA ACA CGA ACC TTT CCT ACG GAG ACC-3', R primer 5'-GCT TGA GTT GTA CGA GAT CCT CGA C-3'. Smad2 F primer 5'-AGC CCG ACG GTA GAG GTA GGA AC-3', R primer 5'-ACT GGC CGA GTG TAT GCC ATG AT-3'. Smad3 F primer 5'-GAA GTC CTG GGA ACT GCG TAG CT-3', R primer 5'-CTC CTG AAG GGT TTA CAG CTT CA-3'. Smad4 F primer 5'-CAG GTG GCT GGT CGG AAA GGA AT-3', R primer 5'-TGG

TGG AGA GGC ATA TTA GGA GA -3'. Smad7 F primer 5'-CCG AGC AGG CGT CCG TAC ATA GT-3', R primer 5'-ACT ATG GCA GCG GGA GAC AGG TG-3'. ERK1 F primer 5'-TTT TCG CAT ATC TCA CTC CAT AGC-3', R primer 5'-ATC AGC TGC TAC AGC CGT ACC TT-3'. ERK2 F primer 5'-TGC ACC GTG ACC TCA AGC CTT CC-3', R primer 5'-CAG AGC CTC TTC ATC ATC AAT CG-3'. GAPDH F primer 5'-TCC ACG TCC CTG TTG CAC TAG-3', R primer 5'-CGA CAG ACG ATG CGA TCAC T-3'. Annealing temperature: TGF- $\beta$ 1 65 °C, Smad2 60 °C, Smad3 55 °C, Smad4 60 °C, Smad7 65 °C, ERK1 65 °C, ERK2 58 °C, GAPDH 60 °C; PCR cycle from the second step cycle 30 to 35 cycles. According to the RT-PCR experimental procedure, changes in TGF- $\beta$ 1, Smad2, Smad3, Smad4, Smad7, ERK1, and ERK2 mRNA were observed in the synovial membrane and lung tissue, and the ratio to the internal reference GAPDH was applied to determine the relative expression.

#### Western blotting of TGF- $\beta$ /Smad and ERK pathway-associated proteins in synovial and lung tissues

After extraction of total protein from the synovial membrane and lung tissue, changes in each protein were detected by immunoblotting. The X-ray film was photographed by a scanner. Protein bands were analyzed by Band Scan software to calculate the gray value. The ratio of the gray values to the  $\beta$ -actin gray value as the internal reference was used to determine relative expression levels of T $\beta$ RI, T $\beta$ RII, Smad2/3, p-Smad2/3, Smad4, Smad7, ERK1/2, and p-ERK1/2 proteins.

### Statistics

The SPSS 18.0 software package was used for statistical analyses. The experimental data were expressed. Datasets were tested for normality. The t-test was used for comparison between groups. Correlations were determined by Spearman's analysis. The level of significance was  $P < 0.05$ .

## Results

### Joint swelling and changes in lung functions

At 6–8 hours after adjuvant injection, the right hind toes of the MC group showed redness and swelling, and the skin was tight and had local thermal sensation. At 2–3 days, swelling of the toes was aggravated. At 6–7 days, the toe was partially ulcerated. Compared with the NC group, swelling of the toes in the MC group was increased significantly and pulmonary function parameters FEV1, FEF50, FEF75, MMF, and PEF were significantly lower,  $P < 0.01$  (Figure 1 and Table 1).

### Joint and lung pathologies

Articular observations revealed that the synovial



**Figure 1.** Changes of Joint swelling in Rats. A: MC group B: NC Group.

**Table 1.** Changes in lung function (n=10,  $\bar{x} \pm S$ ).

Group	lung function parameters						
	FVC	FEV <sub>1</sub>	FEF <sub>25</sub>	FEF <sub>50</sub>	FEF <sub>75</sub>	MMF	PEF
NC	6.09±2.04	68.6±16.38	45.2±26.21	39.4±16.84	37.8±15.87	39.2±15.74	39.5±14.85
MC	5.37±1.70	55.7±15.76 <sup>ΔΔ</sup>	40.7±18.85	27.0±13.07 <sup>ΔΔ</sup>	20.3±12.31 <sup>ΔΔ</sup>	28.5±17.96 <sup>ΔΔ</sup>	29.6±12.57 <sup>ΔΔ</sup>

Note: <sup>Δ</sup>P < 0.05, <sup>ΔΔ</sup>P < 0.01, vs NC. FEF25, FEF50, The lung function parameter FVC unit is ml, FEV1, FEF75, MMF, PEF unit is ml/s.

tissue of rats in the NC group was clear, the synovial membrane was free of hypertrophy and protrusion, and there was no inflammatory cell infiltration. Synovial cells had clear boundaries and less stratification (one to two layers). The articular surface was flat and intact, and the articular cartilage, subchondral bone, and peripheral tendon were structurally intact. In the MC group, a large amount of inflammatory cell infiltration was observed in the joint synovium, which was mostly eosinophils and neutrophils. Increased synovial blood vessels, synovial tissue hyperplasia, and villous processes were observed, and part of the synovial tissue was embedded in the joint cavity. The lining of synovial cells was increased (4–5 layers) and had thickened. The articular surface was blurred, the surface of the articular cartilage was exfoliated or absent, and some articular cartilage was observed to form vasospasm.

Observations of lung tissue showed that the lung tissue structure of the NC group was clear, the structure of the alveoli was regular, and no obvious pathological changes were observed. In the MC group, the alveolar structure of the lung tissue was irregular, the alveolar space was atrophied or disappeared, and some of the lungs were had changed substantially. The lung interval had widened and a large number of inflammatory cells had infiltrated into the interstitium. The inflammatory cells were mainly neutrophils, and lymphoid were rare. Cells, mononuclear macrophages, and alveolar epithelial cells had proliferated, and fibroblasts had proliferated occasionally (Figures 2-3).

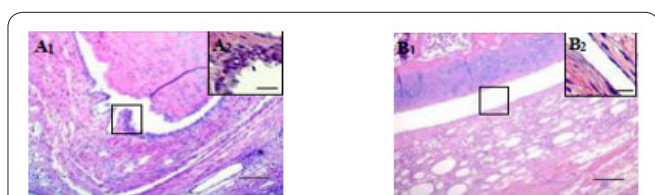


**Figure 2.** Observation of rat synovial membrane under a light microscope. Note: A to B are MC group and NC group respectively; A1 to B1 are ×200, and A2 to B2 are ×400.

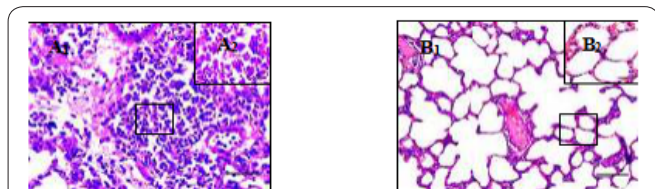


**Figure 3.** Observation of lung tissue in each group of rats under a light microscope. Note: A to B are MC group and NC group respectively; A1 to B1 are ×200, and A2 to B2 are ×400.

**Synovial and lung ultrastructural observations**

Ultrastructural observations of the synovial membrane indicated that the NC group had no deformation or swelling of mitochondria, rich endoplasmic reticulum, a clear nuclear membrane boundary, uniform chromatin distribution, and regular arrangement of condyles. Synovial cells of the MC group were deformed and swollen, mitochondria are swollen and destroyed, the rough endoplasmic reticulum was reduced, the nuclear membrane was incomplete and the boundary was unclear, and chromatin was unevenly distributed.

Ultrastructural observations of type II alveolar cells showed no significant abnormalities in the NC group. The cell membrane boundary of type II alveolar cells in the MC group was unclear. Microvilli of cells were reduced, the basement membrane of the pulmonary capillaries was edematous, and nuclei were irregular or condensed. The nuclear chromatin edge was aggregated, and the lamellar body was reduced and evacuated. Mitochondria in the cytoplasm were obviously swollen, and alveolar septal fibroblasts had proliferated in individual lung tissues together with collagen fibers occasionally. The ultrastructural changes of type II alveolar cells suggested that pulmonary interstitial fibrosis was secondary in the arthritis model (Figure 4-5).

**Changes in cytokines, growth factors, and Th cells**

Compared with the NC group, cytokines IL-1β and IL-4 were increased significantly, cytokines IFN-γ and IL-10 were decreased, and the Th1/Th2 cell ratio was

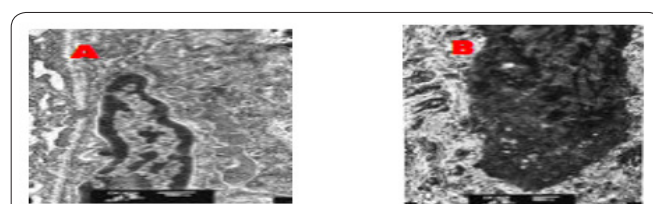


**Figure 4.** Synovial tissue of rats in each group under an electron microscope. Note: A~B was the ultrastructure of synovial cells in the NC group, MC group (×5,000).

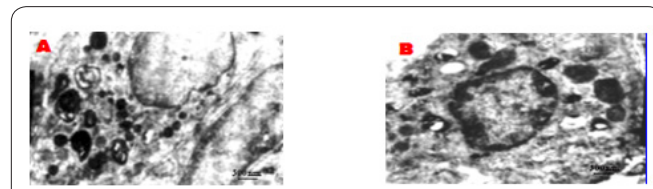


**Figure 5.** Observation of lung tissue in each group of rats under electron microscope. A~B is the ultrastructure of type II alveolar epithelial cells in the NC group and MC group (×5,000).

**Table 2.** Comparison of serum inflammatory cytokines and Th1/Th2 cells ( $\bar{x} \pm S$ , pg/ml)

Group	IL-1β	IL-4	IFN-γ	IL-10	Th1/Th2
NC	32.1±9.46	30.5±13.14	69.9±11.65	106.8±21.24	1.66±0.72
MC	82.5±23.78 <sup>ΔΔ</sup>	44.8±17.72	31.2±7.45 <sup>ΔΔ</sup>	51.8±16.42 <sup>ΔΔ</sup>	0.47±0.19 <sup>ΔΔ</sup>

Note: <sup>Δ</sup>P < 0.05, <sup>ΔΔ</sup>P < 0.01, vs NC.

**Table 3.** Comparison of growth cytokines in serum ( $n=10, \bar{x} \pm s$ , pg/ml).

Group	TGF- $\beta$ 1	CTGF	FGF
N C	156.2 $\pm$ 32.47	78.9 $\pm$ 14.17	35.6 $\pm$ 11.36
M C	192.4 $\pm$ 46.38 <sup>AA</sup>	96.7 $\pm$ 32.54 <sup>A</sup>	25.1 $\pm$ 22.43 <sup>A</sup>

Note: <sup>A</sup> $P < 0.05$ , <sup>AA</sup> $P < 0.01$ , vs NC.

**Table 4.** Comparison of TGF- $\beta$ 1/Smad mRNA in synovial tissue ( $n=8, \bar{x} \pm s$ ).

Group	TGF- $\beta$ 1	Smad2	Smad3	Smad4	Smad7
N C	0.53 $\pm$ 0.27	0.52 $\pm$ 0.17	0.46 $\pm$ 0.16	0.31 $\pm$ 0.15	0.67 $\pm$ 0.28
M C	0.81 $\pm$ 0.19 <sup>AA</sup>	0.63 $\pm$ 0.24 <sup>A</sup>	0.62 $\pm$ 0.21 <sup>AA</sup>	0.43 $\pm$ 0.14 <sup>A</sup>	0.39 $\pm$ 0.19 <sup>AA</sup>

Note: <sup>A</sup> $P < 0.05$ , <sup>AA</sup> $P < 0.01$ , vs NC.

**Table 5.** Expression of TGF- $\beta$ 1/Smad mRNA in lung tissue ( $n=8, \bar{x} \pm s$ ).

Group	TGF- $\beta$ 1	Smad2	Smad3	Smad4	Smad7
N C	0.41 $\pm$ 0.18	0.48 $\pm$ 0.17	0.78 $\pm$ 0.26	0.31 $\pm$ 0.18	0.60 $\pm$ 0.17
M C	0.58 $\pm$ 0.13 <sup>A</sup>	0.61 $\pm$ 0.24 <sup>A</sup>	1.01 $\pm$ 0.34 <sup>A</sup>	0.42 $\pm$ 0.15 <sup>A</sup>	0.50 $\pm$ 0.24 <sup>A</sup>

Note: <sup>A</sup> $P < 0.05$ , <sup>AA</sup> $P < 0.01$ , vs NC.

**Table 6.** Changes of ERK1 and ERK2 mRNA in synovial membrane and lung tissue ( $n=8, \bar{x} \pm s$ ).

Group	synovial		lung	
	ERK1	ERK2	ERK1	ERK2
N C	0.47 $\pm$ 0.13	0.62 $\pm$ 0.18	0.43 $\pm$ 0.16	0.59 $\pm$ 0.16
M C	0.51 $\pm$ 0.17	1.08 $\pm$ 0.27 <sup>AA</sup>	0.52 $\pm$ 0.12 <sup>A</sup>	1.12 $\pm$ 0.27 <sup>AA</sup>

Note: <sup>A</sup> $P < 0.05$ , <sup>AA</sup> $P < 0.01$ , vs NC.

decreased in the MC group,  $P < 0.05$  or  $P < 0.01$ . In addition, compared with the NC group, the expression of TGF- $\beta$ 1 and CTGF was increased, and FGF was decreased in the MC group,  $P < 0.01$  (Tables 2-3).

**Changes in TGF- $\beta$ 1 and Smad mRNA expression of synovial and pulmonary tissues**

RT-PCR showed that the expression of TGF- $\beta$ 1, Smad2, Smad3, and Smad4 mRNAs in the synovium of the MC group was higher than that in the NC group. Expression of Smad7 mRNA was decreased,  $P < 0.05$  or  $P < 0.01$ , and that of TGF- $\beta$ 1, Smad2, Smad3 and Smad4 mRNAs was increased in lung tissue of the MC group. See Table 4-5.

**Changes in ERK1/2 mRNA expression of synovial and lung tissues**

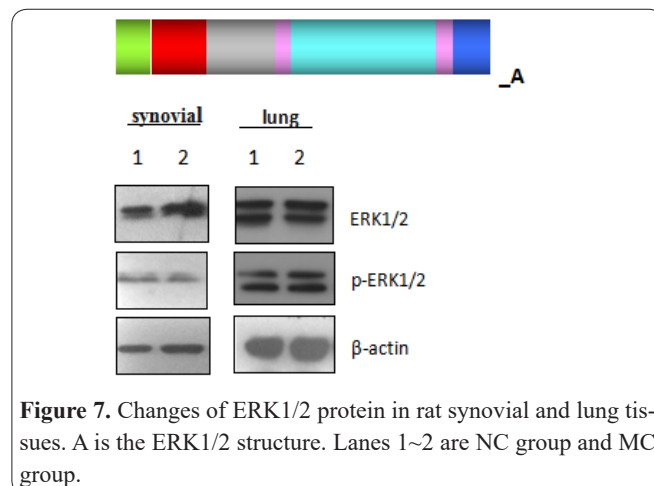
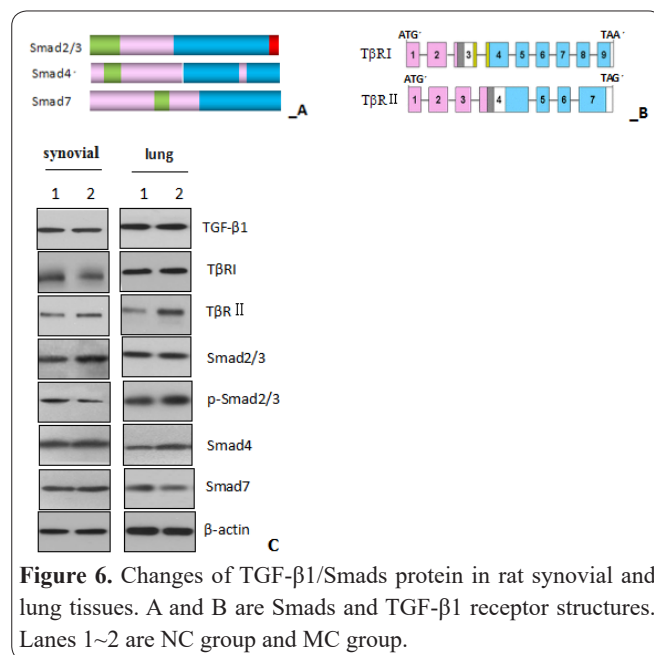
Compared with the NC group, the expression of ERK1/2 mRNA was increased in the synovial membrane and expression of ERK1/2 mRNAs was increased in lung tissue of the MC group,  $P < 0.01$  or  $P < 0.05$  (Table 6).

**Expression of TGF- $\beta$ 1 and Smad proteins in synovial and pulmonary tissues**

Immunoblotting showed that the levels of TGF- $\beta$ 1, T $\beta$ R I, T $\beta$ R II, Smad2/3, p-Smad2/3, and Smad4 were higher and the Smad7 protein level was lower in the MC group than in the NC group,  $P < 0.05$  or  $P < 0.01$  (Figure 6).

**Changes of ERK1/2 and p-ERK1/2 proteins in the synovial membrane and lung tissue**

Compared with the NC group, p-ERK1/2 proteins were significantly increased in the synovial membrane,  $P < 0.01$ , and lung tissue of the MC group,  $P < 0.05$  or



P<0.01 (Figure 7).

### Correlation analysis

Correlation analysis between arterial lung function parameters and TGF- $\beta$ 1/Smads showed that FEF75 was negatively correlated with *TGF- $\beta$ 1* and *Smad3* mRNAs. FEV1 was negatively correlated with *TGF- $\beta$ 1* mRNA, *ERK2* mRNA, and TGF- $\beta$ 1 protein. FEF25 was negatively correlated with Smad4 and p-ERK1/2 proteins. FEF50 was negatively correlated with T $\beta$ RII protein. There was a negative correlation between FEF75 and T $\beta$ RI, Smad2/3, p-Smad2/3, and ERK1/2 proteins, P< 0.05. MMF was negatively correlated with Smad2/3 and p-ERK1/2 proteins, P< 0.05. There was a negative correlation between PEF and TGF- $\beta$ 1 protein, P<0.05. FEF50 was positively correlated with Smad7 mRNA, and MMF was positively correlated with Smad7 protein, P< 0.05.

Correlation analysis between TGF- $\beta$ 1/Smads and ERK1/2 showed that *ERK1* mRNA was positively correlated with *Smad3* mRNA and T $\beta$ RII protein, P< 0.05. *ERK2* mRNA was positively correlated with p-Smad2/3, P< 0.05. ERK1/2 protein was positively correlated with *Smad2* mRNA and Smad4 protein, P< 0.05. p-ERK1/2 proteins were positively correlated with *Smad4* mRNA and p-Smad2/3 proteins, P< 0.05. p-ERK1/2 was negatively correlated with Smad7 protein, P< 0.05 (Tables 7-8).

### Discussion

RA is an autoimmune disease described by joint lesions, which can affect multiple organs (21-22). Moreover, through the blood flow and internal environment, lungs can detrimentally affect the whole body because of the deterioration of the internal environment, resul-

**Table 7.** Relationship between lung function and TGF- $\beta$ 1/Smads pathway in lung tissue.

index	FVC	FEV <sub>1</sub>	FEF <sub>25</sub>	FEF <sub>50</sub>	FEF <sub>75</sub>	MMF	PEF
<b>mRNA</b>							
<i>TGF-<math>\beta</math>1</i>	-0.145	-0.395*	-0.089	-0.301	-0.383*	-0.217	0.174
<i>Smad2</i>	-0.015	-0.214	-0.047	-0.278	-0.103	-0.267	0.115
<i>Smad3</i>	0.045	-0.156	-0.217	-0.185	-0.421*	-0.164	0.086
<i>Smad4</i>	-0.154	-0.405*	0.174	-0.242	-0.264	-0.265	-0.145
<i>Smad7</i>	0.186	0.097	0.135	0.433*	0.143	-0.067	0.412*
<i>ERK1</i>	-0.105	-0.019	-0.154	-0.078	-0.313	-0.201	0.007
<i>ERK2</i>	-0.187	-0.405*	0.074	-0.232	-0.095	-0.185	-0.283
<b>protein</b>							
TGF- $\beta$ 1	-0.117	-0.396*	0.106	0.064	-0.266	-0.201	-0.391*
T $\beta$ RI	0.074	-0.145	-0.095	-0.226	-0.406*	-0.184	0.067
T $\beta$ RII	-0.096	-0.224	0.083	-0.405*	-0.165	0.066	-0.195
Smad2/3	-0.135	0.033	0.124	-0.213	-0.445*	-0.442*	-0.209
p-Smad2/3	-0.168	-0.245	0.036	-0.069	-0.399*	-0.118	-0.206
Smad4	0.039	-0.051	-0.397*	-0.296	-0.059	-0.247	-0.163
Smad7	0.108	0.186	0.258	0.217	0.024	0.407*	0.105
ERK1/2	-0.057	-0.305	0.006	0.064	-0.466*	-0.301	-0.091
p-ERK1/2	0.274	-0.045	-0.395*	-0.154	-0.168	-0.439*	0.084

Note: The abscissa is associated with the ordinate index, \* P < 0.05.

**Table 8.** Relationship between Smads and ERK pathways in lung tissue (r).

index	mRNA		protein		
	ERK1	ERK2	ERK1/2	p-ERK1/2	
<b>Smads mRNA</b>	<i>TGF-<math>\beta</math>1</i>	0.165	-0.061	-0.089	0.304
	<i>Smad2</i>	-0.003	0.272	0.397*	0.272
	<i>Smad3</i>	0.398*	0.308	0.277	0.184
	<i>Smad4</i>	0.157	-0.106	0.174	0.414*
	<i>Smad7</i>	-0.162	0.097	-0.135	-0.239
<b>Smads protein</b>	TGF- $\beta$ 1	0.217	0.196	0.176	0.064
	T $\beta$ RI	-0.007	0.245	0.109	0.388 *
	T $\beta$ RII	0.386*	-0.184	0.009	-0.247
	Smad2/3	0.065	0.066	0.024	0.207
	p-Smad2/3	0.311	0.442*	0.036	0.409*
	Smad4	0.033	-0.052	0.397*	0.275
	Smad7	-0.169	-0.061	0.158	-0.423*

Note: The abscissa is associated with the ordinate index, \* P < 0.05.

ting in changes in the respiratory system. RA lung lesions can lead to interstitial lung disease, rheumatoid nodules, and pleural hypertrophy (23-24). The early clinical manifestations of RA lung damage are generally non-specific, and lung functions decline earlier than clinical symptoms and lung CT changes (25-26). The pulmonary dysfunction rate in RA patients was 48.6% in patients with decreased lung functions (27).

Based on the abovementioned characteristics of RA lung function changes, lung function changes were observed in RA model rats (28-30). According to the results of this study, the toe swelling was elevated in the MC group, while pulmonary functions such as FEV1, FEF50, FEF75, MMF, and PEF were decreased. This indicates that rats' lung function changes at the same time as joint inflammation occurs in RA. Therefore, by observing the lung functions of the arthritis model, the characteristics of RA lung lesions were simulated. The results of this study found Ultrastructural observations of type II alveolar cells in RA rats by electron microscopy showed changes. Therefore, the pulmonary inflammatory response of RA rats directly led to damage to the lung tissue, resulting in decreases in lung functions. The changes in RA cytokines and growth factors in this study indicated that the decrease in lung functions of RA rats may be related to an imbalance of inflammatory cytokine and growth factor expression. When the inflammatory cytokine IL-1 $\beta$  was increased in RA rats, it inhibited the secretion of anti-inflammatory cytokines, resulting in decreased expression of IL-10 and increased inflammatory response, leading to damage of lung tissue. Th1 and Th2 cells secrete different cytokines. When the Th1/Th2 cell ratio is imbalanced, Th1 cell predominance leads to excessive secretion of IL-4, while Th2 cells secrete IFN- $\gamma$ , which leads to pulmonary interstitial fibrosis. In this study, a decrease in lung functions occurred and the expression of growth factors TGF- $\beta$ 1, CTGF, and FGF became disordered, which aggravated pulmonary fibrosis, and the lung functions of RA rats were decreased further.

Correlation analysis showed that FEV1 was negatively correlated with *TGF- $\beta$ 1 mRNA* and protein in arthritic rats, FEF25 was negatively correlated with Smad4 protein, and FEF50 was negatively correlated with the T $\beta$ RII protein. There was a negative correlation between Smad2/3 protein and a negative correlation between PEF and TGF- $\beta$ 1 protein. FEF50 and MMF were positively correlated with *Smad7 mRNA*. FEV1 was negatively correlated with *ERK2 mRNA*, and FEF25 was negatively correlated with p-ERK1/2 protein. FEF75 and MMF were negatively correlated with ERK1/2 and p-ERK1/2, respectively. Analysis of the correlations between lung functions and the Smad pathway in the arthritis model suggested that activation of the TGF- $\beta$ 1/Smad pathway decreased RA lung functions. Based on the correlation results, the Smad pathway bound to T $\beta$ R1 through the TGF- $\beta$ 1 promoter, thereby phosphorylating T $\beta$ R1 and forming a trimer complex. The complex further phosphorylated Smad2/3 and activated Smad2/3 bound to to the TGF- $\beta$ 1 receptor trimer, and under the assistance of Smad4, entered the nucleus and participated in transcriptional activities, leading to the occurrence of pulmonary interstitial fibrosis and resulting in a decrease in lung functions (31-32).

The pulmonary function parameter FEV1 was associated with ERK, and activation of the ERK1/2 signaling pathway also decreased lung functions in RA rats. After phosphorylation, ERK1/2 promotes cell proliferation and differentiation. Correlation analysis showed that *ERK1 mRNA* was positively correlated with *Smad3 mRNA* and T $\beta$ RII protein, *ERK2 mRNA* was positively correlated with p-Smad2/3, and ERK1/2 protein was positively correlated with *Smad2 mRNA*, Smad4 protein. When the ERK pathway is activated, ERK1/2 translocates from the cytoplasm into the nucleus, transducing the signal from the membrane surface receptor (33-35). ERK1/2 then binds to transcription factors, such as calnexin and cytoskeletal proteins, in the nucleus to induce epithelial-to-mesenchymal transition in the cells, which converts lung fibroblasts into myofibroblasts, eventually leading to a decrease in lung functions during arthritis. This study found that the mRNA expression of ERK1 and ERK2 in lung tissue was increased when lung function parameters were decreased in the arthritis model. Protein expression of ERK1/2 and p-ERK1/2 was also elevated in lung tissue. These observations indicated that the reduction of lung functions in the arthritis model was closely related to the activation of the ERK1/2 pathway. Similar to the Smad pathway, the ERK1/2 pathway also bound to transcription factors in the nucleus to exert biological effects, leading to the occurrence of pulmonary interstitial fibrosis (36).

Correlation analysis of TGF- $\beta$ 1/Smad and ERK1/2 pathways in lung tissue of the arthritis model showed that decreased lung functions may be related to their activation. Therefore, crosstalk of Smad and ERK1/2 pathways may have resulted in the decreased lung functions of the arthritis model. This study found that, when the lung functions of the arthritis model were reduced, expression of ERK1/2 genes was increased in the lungs and synovium, and protein expression of ERK1/2 and p-ERK1/2 was also increased, thereby verifying the RA rats. Therefore, decreased lung functions may be associated with the activation of ERK1/2.

### Acknowledgments

This work was supported by grants from the National Natural Science Foundation of China (81973655), Ministry of Science and Technology National Key Research and Development Plan for Traditional Chinese Medicine Modernization Research Special Project (2018YFC1705204), National Training Program for Innovative Key Talents of Traditional Chinese Medicine (Guo TCM Letter [2019] 128), Anhui Province Provincial Quality Engineering Teaching Research Project (2018jyxm1068), Funding for Graduate Innovation Program of Anhui University of Chinese Medicine (2019YJG013). We thank Mitchell Arico from Edanz Group ([www.edanzediting.com/ac](http://www.edanzediting.com/ac)) for editing a draft of this manuscript.

### Conflict of Interest

The authors declare that they have no competing interests.

### Author's contribution

W.L. and L.J. conceived and designed the study. The experiment was conducted by G.Y., F.H.X., Z.L., and L.Z.

analysed the data. W.L. wrote the manuscript including a figure by a critical discussion with H.C.B, C.X., L.L. and L.T.Y. All authors contributed to the final manuscript.

## References

- Valerio F, Daccord C, Letovanec I, Hügle T, Lazor R. Rheumatoid arthritis-associated interstitial lung disease : new genetic data and therapeutic perspectives. *Rev Med Suisse* 2019; 15(641): 536-541.
- Sambataro G, Sambataro D, Pignataro F, Torrisi SE, Vancheri A, Pavone M, Palmucci S, Papa ND, Vancheri, C. Interstitial Lung Disease in Patients with Polymyalgia Rheumatica: A case series. *Respir Med Case Rep* 2018; 26:126-130.
- Li W, Jia MX, Wang JH, Lu JL, Deng J, Tang JX, Liu C. Association of MMP9-1562C/T and MMP13-77A/G polymorphisms with non-small cell lung cancer in southern Chinese population. *Biomol* 2019; 9(3), 107-119.
- Lou Y, Shi J, Guo D, Qureshi AK, Song L. Function of PD-L1 in antitumor immunity of glioma cells. *Saudi J Biol Sci* 2017; 24(4): 803-807.
- Lou Y, Yang J, Wang L, Chen X, Xin X, Liu Y. The clinical efficacy study of treatment to Chiari malformation type I with syringomyelia under the minimally invasive surgery of resection of Submeningeal cerebellar Tonsillar Herniation and reconstruction of Cisterna magna. *Saudi J Biol Sci* 2019; 26(8): 1927-1931.
- Bes C. Comprehensive review of current diagnostic and treatment approaches to interstitial lung disease associated with rheumatoid arthritis. *Eur J Rheumatol* 2018; 6(3):146-149.
- Endo Y, Koga T, Tsutsui S, Ashizawa K, Kawashiri S, Kawakami A. Lung consolidation and mediastinal lymphadenopathy in patients with early anti-citrullinated protein antibody-positive rheumatoid arthritis. *Clin Exp Rheumatol* 2019; 37(3):517-518.
- Kechaou I, Boukhris I. Senile rheumatoid arthritis associated with rheumatoid lung: a caricatural observation. *Pan Afr Med J* 2018; 30:253.
- Nie Y, Luo F, Wang L, Yang T, Shi L, Li X, Shen J, Xu W, Guo T, Lin Q. Anti-hyperlipidemic effect of rice bran polysaccharide and its potential mechanism in high-fat diet mice. *Food Func* 2017; 8(11): 4028-4041.
- Valerio F, Daccord C, Letovanec I, Hügle T, Lazor R. Rheumatoid arthritis-associated interstitial lung disease : new genetic data and therapeutic perspectives. *Rev Med Suisse* 2019; 15(641):536-541.
- Krause A, Rubbert-Roth A. Pulmonary involvement in rheumatoid arthritis. *Z Rheumatol* 2019; 78(3):228-235.
- Mori S, Koga Y, Sugimoto M. Different risk factors between interstitial lung disease and airway disease in rheumatoid arthritis. *Respir Med* 2012; 106(11):1591-1599.
- Lou Y, Guo D, Zhang H, Song L. Effectiveness of mesenchymal stem cells cultured by hanging drop vs. conventional culturing on the repair of hypoxic-ischemic-damaged mouse brains, measured by stemness gene expression. *Open Life Sci* 2016; 11(1): 519-523.
- Leonel D, Lucia C, Muñoz A, Martha-Alicia H, Blanca M. Pulmonary function test: its correlation with pulmonary high-resolution computed tomography in patients with rheumatoid arthritis. *Rheumatol Int* 2012; 32(7):2111-2116.
- Liang Y, Lin Q, Huang P, Wang Y, Li J, Zhang L, Cao J. Rice Bioactive Peptide Binding with TLR4 To Overcome H2O2-Induced Injury in Human Umbilical Vein Endothelial Cells through NF- $\kappa$ B Signaling. *J Agri Food Chem* 2018; 66(2): 440-448.
- Wang L, Lin Q, Yang T, Liang Y, Nie Y, Luo Y, Luo F. Oryzanol modifies high fat diet-induced obesity, liver gene expression profile, and inflammation response in mice. *J Agri Food Chem* 2017; 65(38): 8374-8385.
- Guo T, Lin Q, Li X, Nie Y, Wang L, Shi L, Luo F. Octacosanol attenuates inflammation in both RAW264. 7 macrophages and a mouse model of colitis. *J Agri Food Chem* 2017; 65(18), 3647-3658.
- Chen X, Xu Y, Meng L, Chen X, Yuan L, Cai Q, Shi W, Huang G. Non-parametric partial least squares–discriminant analysis model based on sum of ranking difference algorithm for tea grade identification using electronic tongue data identify tea grade using e-tongue data. *Sens Actuators B Chem* 2020; 127924.
- Nie Y, Luo F, Lin Q. Dietary nutrition and gut microflora: A promising target for treating diseases. *Trends Food Sci Tech* 2018; 75, 72-80.
- Ren Y, Jiao X, Zhang L. Expression level of fibroblast growth factor 5 (FGF5) in the peripheral blood of primary hypertension and its clinical significance. *Saudi J Biol Sci* 2018; 25(3), 469-473.
- Marcucci E, Bartoloni E, Alunno A, Leone MC, Cafaro G, Lucchioli F, Valentini V, Valentini E, La Paglia GMC, Bonifacio AF, Gerli, R. Extra-articular rheumatoid arthritis. *Rheumatism* 2018; 70(4):212-224.
- Cojocaru M, Cojocaru IM, Silosi I, Vrabie CD, Tanasescu R. Extra-articular Manifestations in Rheumatoid Arthritis. *Medica* 2010; 5(4):286-291.
- Gregersen PK, Gravallesse EM. Breathing New Life into Interstitial Lung Disease in Rheumatoid Arthritis. *N Engl J Med* 2018; 379(23):2265-2266.
- Prete M, Racanelli V, Digiglio L, Vacca A, Dammacco F, Perosa F. Extra-articular manifestations of rheumatoid arthritis: An update. *Autoimmun Rev* 2011; 11(2):123-131.
- Cottin V. Pragmatic prognostic approach of rheumatoid arthritis-associated interstitial lung disease. *Eur Respir J* 2010; 35(6):1206-1208.
- Habib HM, Eisa AA, Arafat WR, Marie MA. Pulmonary involvement in early rheumatoid arthritis patients. *Clin Rheumatol* 2011; 30(2): 217-221.
- Martinez JA. Pulmonary impairment in rheumatoid arthritis. *Rev Bras Reumatol* 2011; 51(4):295-296, 298.
- Song LN, Kong XD, Wang HJ, Zhan LB. Establishment of a Rat Adjuvant Arthritis-Interstitial Lung Disease Model. *Biomed Res Int* 2016; 2970783.
- Wan L, Liu J, Huang C, Wang Y, Zheng L. Effect of xinfeng capsule on pulmonary function in a adjuvant arthritis rat model. *J Tradit Chin Med* 2014; 34(1):76-85.
- Wan L, Liu J, Huang CB, Wang Y, Lei L, Liu L, Cheng YY, Feng YX. Effect of tripterygium glycosides on pulmonary function in adjuvant arthritis rats. *J Chin Med Assoc* 2013; 76(12):715-23.
- Luo L, Wang CC, Song XP, Wang HM, Zhou H, Sun Y, Wang XK, Hou S, Pei FY. Suppression of SMOC2 reduces bleomycin (BLM)-induced pulmonary fibrosis by inhibition of TGF- $\beta$ 1/SMADs pathway. *Biomed Pharmacother* 2018; 105:841-847.
- Liu YY, Shi Y, Liu Y, Pan XH, Zhang KX. Telomere shortening activates TGF- $\beta$ /Smads signaling in lungs and enhances both lipopolysaccharide and bleomycin-induced pulmonary fibrosis. *Acta Pharmacol Sin* 2018; 39(11):1735-1745.
- Tao W, Sun W, Zhu H, Zhang J. miR-205-5p suppresses pulmonary vascular smooth muscle cell proliferation by targeting MICAL2-mediated Erk1/2 signaling. *Microvasc Res* 2019;124:43-50.
- Yaykasli KO, Hatipoglu OF, Yaykasli E, Yildirim K, Kaya E, Ozsahin M, Uslu M, Gunduz E. Leptin Induces ADAMTS-4, ADAMTS-5, and ADAMTS-9 Genes Expression via Mitogen Activated Protein Kinases and NF- $\kappa$ B in Human Chondrocytes. *Cell Biol Int* 2015; 39(1):104-112.
- Okada M, Yamane M, Yamamoto S, Otani S, Miyoshi K, Sugimoto S, Matsukawa A, Toyooka S, Oto T, Miyoshi S. SPRED2 deficiency may lead to lung ischemia-reperfusion injury via ERK1/2

signaling pathway activation. *Surg Today* 2018; 48(12):1089-1095.

36. Li J, Zhao Z, Liu J, Huang N, Long D, Wang J, Li X, Liu Y. MEK/ERK and p38 MAPK regulate chondrogenesis of rat bone marrow mesenchymal stem cells through delicate interaction with TGF-beta1/Smads pathway. *Cell Prolif* 2010; 43(4):333-43.

37. Hu Y, Li CS, Li YQ, Liang Y, Cao L, Chen LA. Perfluorocarbon

inhibits lipopolysaccharide-induced macrophage inflammatory protein-2 expression and activation of ATF-2 and c-Jun in A549 pulmonary epithelial cells. *Cell Mole Biol* 2016; 62(4): 18-24.

38. Sohn EJ, Kim J, Hwang Y, Im S, Moon Y, Kang DM. TGF-beta suppresses the expression of genes related to mitochondrial function in lung A549 cells. *Cell Mole Boil* 2012; OL1763-1767.